



ESTIMATION OF SEDIMENTARY AQUIFER'S PARAMETERS WITHIN IDAH AND ENVIRONS, PART OF NORTHERN ANAMBRA BASIN, NIGERIA

*Kingsley, O. O. and Kizito, O. M.

Department of Geology, Federal University Lokoja, Lokoja, Kogi State, Nigeria

*Corresponding authors' email: kingsleyicabest@gmail.com

ABSTRACT

Due to increase in population and pollution of surface water, there is high demand for groundwater within the area. As such, this research aimed at investigating the groundwater potential and aquifer protective capacity using vertical electrical sounding (VES) and computation of Dar-Zarrouk parameters. 40 locations were investigated using Schlumberger array, data was analyzed manually and final plot was processed using WinResist. The value of aquifer resistivity and thickness were used to compute the Dar-Zarrouk parameters; final map was produced using Surfer software. VES result showed 4-6 layers. The layers are top soil, lateritic, compacted sandstone, Sandstone/clay/clayey sand, Aquiferous sandstone/sandy clay and highly compacted sandstone/shale. Curve types are AK, K, HA, KH, A, AH, and HK. Aquifer resistivity and thickness values range from 19.6 Ωm to 8986.9 Ωm and 2 m to 84.6 m having mean value of 1769.66 Ωm and 29.52m. Depth to groundwater varies from 6.8 m to 144.6 m indicating shallow and deeper aquifer depth. Longitudinal conductance (Lc) and transverse unit resistance (Tr) value ranges from 0.0052 siemens to 2.9898 siemens and 435.2 Ωm^2 to 584391.4 Ωm^2 , average value of 0.2455 siemens and 52860.83 Ωm^2 . Hydraulic conductivity (K) and transmissivity (T) value ranges from 0.0793 m/day to 24.0759 m/day and 0.3725 m^2/day to 1410.846 m^2/day and mean value of 3.6192 m/day and 122.5311 m^2/day . According to the interpreted result, the research region has moderate to high groundwater potential and poor to good protective capacity. As a result, the outcome can be used as a reference point in groundwater monitoring and management.

Keywords: Sedimentary Aquifers, Groundwater, Northern Anambra Basin, Nigeria

INTRODUCTION

Idah Local Government Area is one of the earliest local government areas established in Igala-land, dating back to 1979, with its creation coinciding with that of Dekina and Ankpa Local Government Areas. It is bounded by Igalamela and Ibaji Local Government Area and River Niger at the east. From the knowledge of field mapping carried out within the study area, Ocheche, Inachalo, Ofu, Emachi and Ega river are tributaries of River Niger, and serves as one of the main rivers that spans through the research region. These rivers are considered to be contaminated due to increase in population and industrialization leading to its unsuitability for drinking and other purposes. Also, in the GRA part of Idah, depth to ground water is very deep while within the main town the depth is intermediate and towards the boundary between Idah and Ibaji environment, boreholes depths are shallow. As a result, the community now depends on groundwater abstracted through hand dug wells and boreholes. Therefore, there is need to investigate the nature of its groundwater and the depth variation that occur in the area.

Accessing water, an essential resource for daily life, hinges on a comprehensive understanding of geological structures, as highlighted by Eyankware and Okeke (2018). Due to its inherent natural characteristics, groundwater has emerged as a crucial and reliable source of water supply across diverse climatic regions worldwide, including tropical areas (Anandhi and Kannan, 2018; Singh et al., 2018; Preeja et al., 2011). Groundwater is one of the most important sources of water supply in settlements especially rural communities and small towns in Nigeria. Currently, over 80% of water provided for small towns for domestic use is extracted from groundwater sources (Adagunodo, 2017a; Kalaivanan et al., 2019).

Accurately understanding the occurrence, movement, and flow direction of groundwater is essential, as it resides within underground geologic formations known as aquifers (Kizito et al., 2023a, 2023b). The characteristics of these aquifers

vary significantly based on factors such as geological settings, rock or sediment types, and stored water volumes (Okoli et al., 2024). Effective environmental management and prevention of overexploitation require insight into groundwater dynamics. Sustainable extraction methods are crucial to prevent adverse environmental impacts like land subsidence and seawater intrusion (Emenike et al., 2018). Excessive groundwater extraction can have severe long-term consequences, including aquifer system degradation and diminished water quality.

The hydro-geo-electrical resistivity technique has been extensively applied in groundwater exploration by researchers, government agencies, and industries, effectively addressing various challenges associated with groundwater exploration (Zohdy et al., 1974; Nigm et al., 2008; Thabit and Al-hameedawie, 2014; Elbarbary et al., 2021; Simon et al., 2022; Obasi et al., 2023; Kizito et al., 2023a; Hudu et al., 2024). Crucial parameters, including hydraulic conductivity, transverse resistance, longitudinal conductance, and transmissivity, play a vital role in evaluating the groundwater potential of a given area (Akidi et al., 2024). Aside the application of pumping test, geoelectric techniques have been widely used in computing the above aquifer parameters through the application of Dar-Zarrouk parameters (Kizito et al., 2023; Obasi et al., 2023; Akidi et al., 2024; Hudu et al., 2024). Despite the importance of evaluating groundwater potentials in the Anambra Basin, previous studies are focused mainly on the geological and hydrological characteristic of the area with limited integration of geophysical data and Dar-Zarrouk parameters. Furthermore, there is scarcity of information on the application of this parameters in estimating sedimentary parameters and evaluating groundwater potential in Idah and environs. This study aims to bridge this knowledge gap by utilizing geophysical data and Dazarouk parameters to evaluate the groundwater potentials in the study area

MATERIALS AND METHODS

Location and Geologic Setting

The study area lies within Latitude N7°03'00'' to 7°11'30'' and Longitude E6°44'00'' to E6°57'00'' and covers a land mass of 433 km². The study area covers Achokpa, Ogbogbo and Idah town within the Idah local Government (Figure 1). The area boasts an efficient drainage system, with notable rivers such as Ocheche, Inachalo, Ofu, Emachi, and Ega, along with streams that occupy expansive valleys. Idah's climate is quintessentially tropical, characterized by two distinct seasons: a wet/rainy season and a dry/summer season. The rainy season, which spans from April to October, is marked by high humidity and intense rainfall, with annual precipitation ranging from 1500-2500mm; the heaviest rainfall occurs between June and July, subsides, and then intensifies again in September (Iloeje, 2001). The local economy is primarily driven by farming and fishing, leveraging its proximity to the River Niger. While there are various small-scale industrial activities, such as bakeries, palm oil mills, and block-making enterprises, the area lacks robust industrial development, as evidenced by the defunct sanitary ware industry established by the state (Bolade et al., 2021).

Geologically, the area comprises the Ajali and Mamu formations within the Northern Anambra Basin of Nigeria (Figure 1). With a significant sediment layer of about 9 km, the Cretaceous Anambra Basin provides the perfect conditions for intricate chemical processes that may result in the creation of commercially viable hydrocarbon reserves (Whiteman, 1982). This roughly triangular basin spans around 40,000 km² located in southern-central Nigeria, extending northwards along the Benue River (Olubayo, 2010). The basin's fill is characterized by facies of the Nkporo Group and the Coal Measures, as described by Nwajide (2013). The Anambra Basin encompasses the sedimentary succession directly overlying the southern Benue Trough's facies, comprising Campanian to early Paleocene lithofacies. This basin hosts a diverse range of economically significant geological materials, including metalliferous minerals, industrial minerals and rocks, and energy/fuel minerals (Nwajide, 2013). The Ajali Sandstone, attributed to fluvial deposition (Onyekuru et al., 2023), is characterized by massive channels filled with fining-upward sequences of conglomeratic sandstones (Nwajide, 2005).

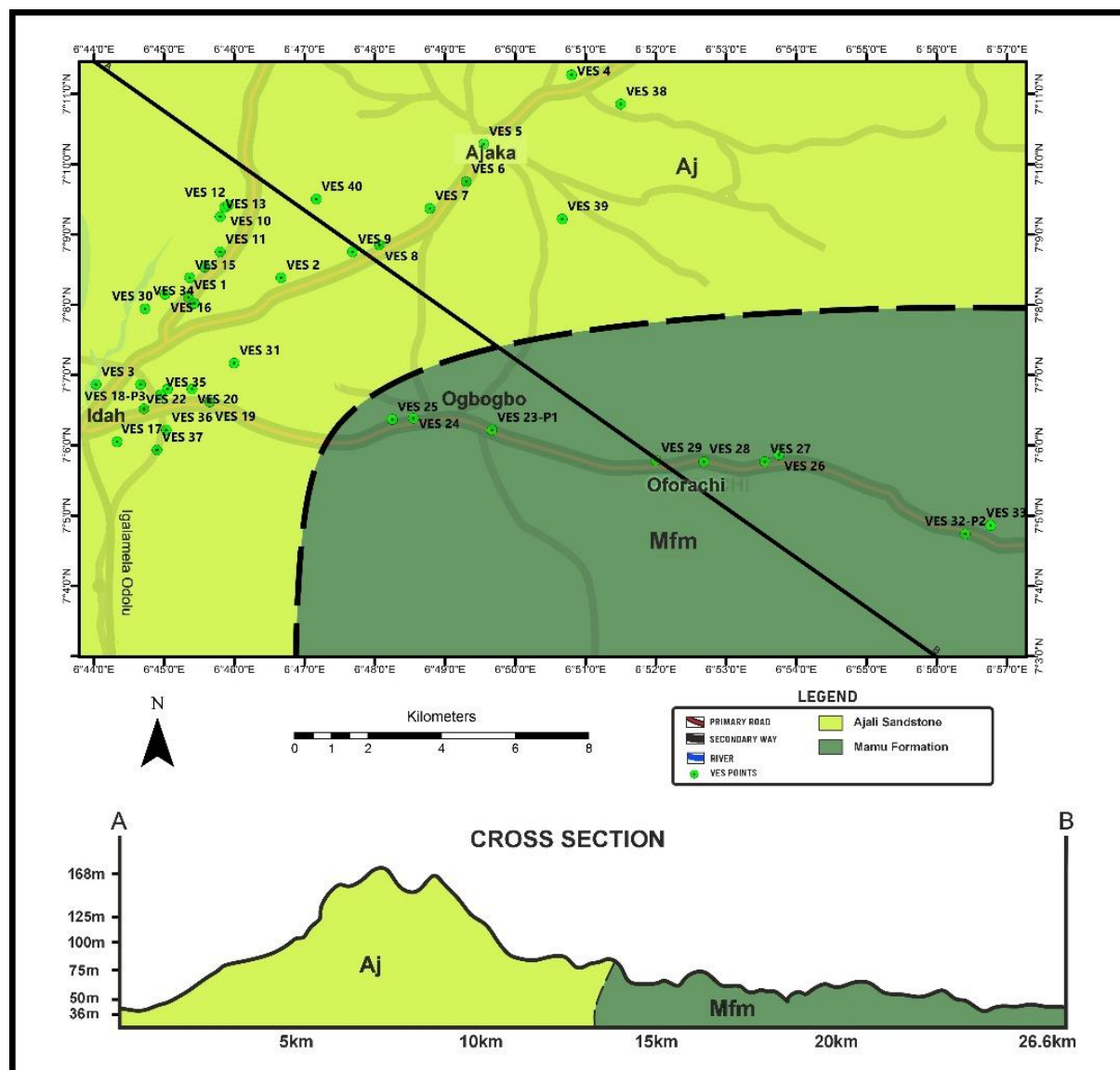


Figure 1: Geology map of the study area

Data Acquisition and Processing

Vertical Electrical Sounding (VES) using Schlumberger electrode configuration was used to obtain subsurface information in forty (40) locations within the study area. Conventionally, Schlumberger array used four electrodes;

two each for current and potential electrodes. These electrodes are pegged to the ground in a horizontal at equidistance based on the prepared data sheet. Figure 2 illustrates how field data is collected and how subsurface currents interact.

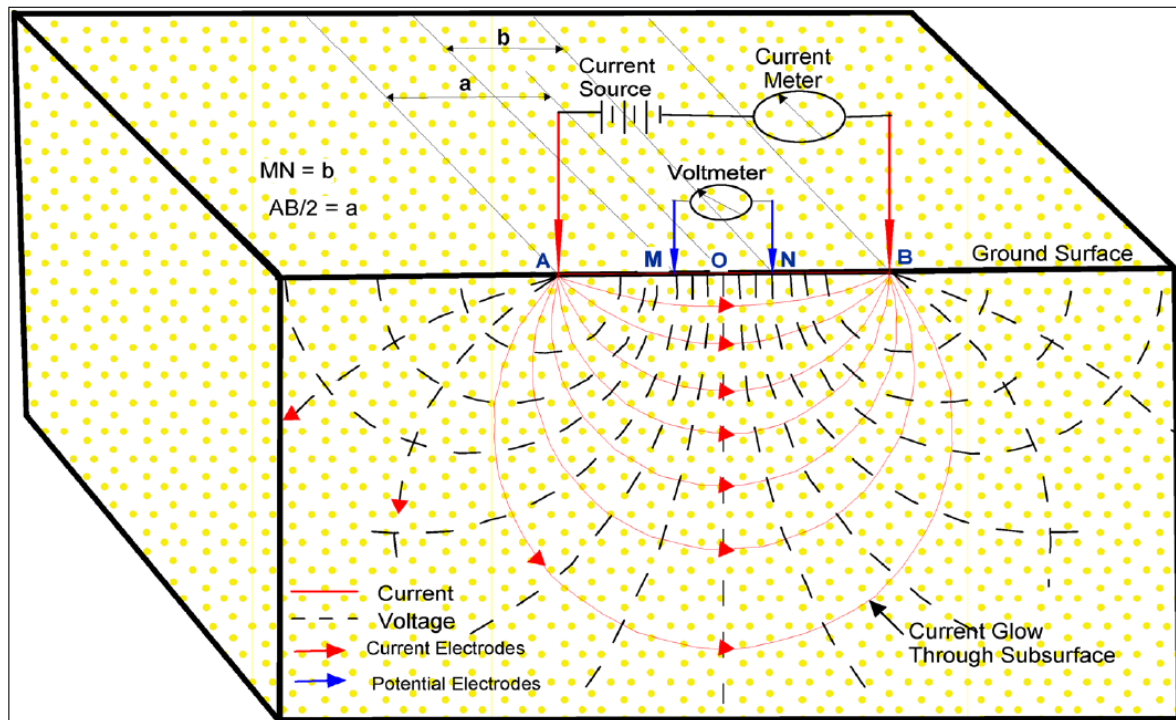


Figure 2: Diagram Illustrating Electrical Resistivity Setup (Adapted from Akiang et al., 2024)

The electrode configurations employed in this study featured a maximum current electrode spacing ($AB/2$) ranging from 1.0m to 200.0m, while the maximum potential electrode spacing ($MN/2$) varied from 0.5m to 15.0m. According to Bernard (2003), Anudu et al. (2014), and Obrike et al. (2022), the depth of investigation for resistivity sounding with the Schlumberger electrode array is roughly 25-33% of the distance between the current electrodes ($AB/2$). Initial estimates of the Vertical Electrical Sounding (VES) data were obtained using the conventional partial curve matching technique, incorporating two-layer master curves and auxiliary point diagrams as described by Orellana and Mooney (1966). These estimated layer resistivities and thicknesses served as starting points for computer-assisted interpretation. Subsequent modeling of the one-dimensional (1-D) VES curves was performed using the WinResist 1.0 software, from which layer resistivity, thickness, and depth were estimated.

Dar-Zarrouk Parameters

In groundwater exploration, the VES approach is frequently employed to ascertain an aquifer's thickness, resistivity, boundary, and depth from its surface (Anudu et al., 2014; Obrike et al., 2022). The Dar-Zarrouk parameters derivable from VES models include; longitudinal conductance and transverse resistance. These parameters made it possible to compute the intrinsic hydraulic properties and aquifer parameters such as hydraulic conductivity and transmissivity, which gives insight regarding the groundwater potentials of existing aquifers in the region. The Dar-Zarrouk parameters and aquifer properties are calculated using the following equations as given by Akpan et al. (2015), Simon et al. (2022),

Obrike et al., 2022), Obasi et al. (2022, 2023), Kizito et al. (2023a, 2023b), Akidi et al. (2024). Contour maps illustrating the spatial distribution of the parameters were generated using Surfer software (version 25.1.229) with the calculated parameter values.

$$\text{Longitudinal conductance (Lc)} = \frac{h}{\rho_a} \text{ (Siemens)} \quad (1)$$

$$\text{Transverse resistance (TR)} = \rho_a h \text{ (ohm} \cdot \text{m}^2) \quad (2)$$

$$\text{Hydraulic conductivity (K)} = 386.40 (\rho_a)^{-0.93283} \text{ (m/day)} \quad (3)$$

$$\text{Transmissivity (T)} = K \times h \text{ (m}^2\text{/day)} \quad (4)$$

Where aquifer thickness and resistivity are denoted by h and ρ_a , respectively.

RESULTS AND DISCUSSION

The geoelectric layer as presented in Table 1 show four (4) to six (6) subsurface lithology with varying resistivity and thickness value. The layer includes the top soil, lateritic clay, compacted sandstone, Sandstone/clay/clayey sand, Aquiferous sandstone/sandy clay and highly compacted sandstone/shale as the case may be. The top soil has resistivity and thickness ranges from 49.7-932.2 Ωm and 0.305.5 m. The thickness and resistivity of lateritic clay range from 7.7-81325 Ωm , while those of compacted sandstone range from 11.0-21702.2 Ωm and 1.1-35.6 m. Sandstone or clayey sand has resistivity value ranges from 7.7-8986.6 Ωm and 10.4-70.8 m, the aquiferous sandstone has resistivity and thickness value ranges from 54-20616.5 Ωm and 6.8-84.6, and the highly compacted sandstone/shale has resistivity ranges from 503.6-51103.2 Ωm . The common examples of the VES curves for few of the location is presented in Figure 3.

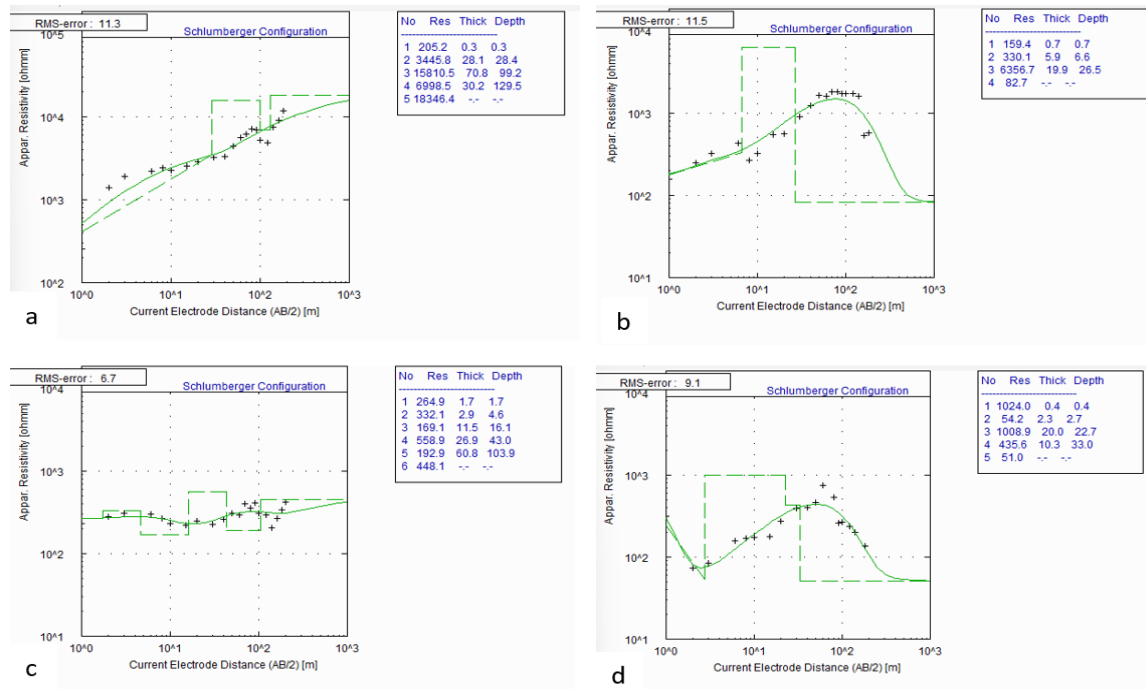


Figure 3: Common Examples of VES Curves for Location (a) 1, (b) 2, (c) 5, and (d) 15

Table 1: Summary of VES Geoelectric Layer Parameters

VES No.	Resistivity (Ωm)	Thickness (m)	Depth (m)	Lithology	Curve Type
1	205.2	0.3	0.3	Top soil	AK
	3445.8	28.1	28.4	Lateritic Clay	
	15810.5	70.8	99.2	Compacted sandstone	
	6998.5	30.2	129.5	Sandstone/aquifer layer	
	18346.4			Sandstone	
2	159.4	0.7	0.7	Top soil	K
	330.1	5.9	6.6	Lateritic Clay	
	6356.7	19.9	26.5	Compacted sandstone	
	82.7			Sandstone/aquifer layer	
3	49.7	1.3	1.3	Top soil	HA
	20.0	3.4	4.7	Lateritic Clay	
	1660.5	10.4	15.1	Compacted sandstone	
	1008.7	4.6	19.8	Sandstone/aquifer layer	
	19458.0			Sandstone	
4	210.6	1.5	1.5	Top soil	KH
	705.4	3.3	4.9	Lateritic Clay	
	237.6	13.6	18.4	Sandstone	
	1388.1	23.6	42.0	Sandstone/aquifer layer	
	23397.4			Sandstone	
5	264.9	1.7	1.7	Top soil	KH
	332.1	2.9	4.6	Lateritic Clay	
	169.1	11.5	16.1	Compacted sandstone	
	558.9	26.9	43.0	Sandstone	
	192.9	60.8	103.9	Sandstone/aquifer layer	
	448.1			Sandstone/shale	
6	267.7	0.4	0.4	Top soil	KH
	2700.7	1.1	1.5	Lateritic Clay	
	139.2	3.7	5.2	Sandstone/aquifer layer	
	4261.7	5.7	10.8	Sandstone	
	10000.0			Compacted Sandstone	

VES No.	Resistivity (Ω m)	Thickness (m)	Depth (m)	Lithology	Curve Type
7	292.6	0.8	0.8	Top soil	A
	1978.3	4.2	5.1	Lateritic Clay	
	1283.9	4.7	9.8	Sandstone/aquifer layer	
	8986.6	5.7	15.5	Sandstone	
	10000.0			Compacted sandstone	
8	932.5	0.5	0.5	Top soil	HA
	60.5	1.3	1.7	Lateritic Clay	
	922.8	1.9	3.6	Sandstone/aquifer layer	
	10365.5	5.2	8.8	Compacted Sandstone	
	12349.0	4.7	13.5	Compacted sandstone	
9	185.5	0.4	0.4	Top soil	KH
	1672.8	1.0	1.4	Lateritic Clay	
	108.8	4.0	5.4	Sandstone/aquifer layer	
	1534.0	4.3	9.7	Compacted Sandstone	
	100000.0			Compacted Sandstone	
10	224.7	4.3	4.3	Top soil	KH
	3214.5	7.7	12.0	Lateritic Clay	
	1520.1	9.3	21.3	Compacted sandstone	
	138.0	22.5	43.8	Sandstone/aquifer layer	
	54.0	34.9	78.7	Sandy clay	
11	366.5	0.4	0.4	Top soil	K
	887.1	5.8	6.2	Lateritic Clay	
	3959.0	21.8	28.0	Compacted sandstone	
	870.8			Sandstone/aquifer layer	
12	602.2	4.2	4.2	Top soil	KH
	1242.2	35.6	39.8	Lateritic Clay	
	330.4	40.3	80.1	Sandy clay	
	596.7	23.2	103.3	Compacted sandstone	
	323.2	39.6	142.9	Sandstone/aquifer layer	
13	506.1			Sandstone	KH
	112.5	0.5	0.5	Top soil	
	8325.5	4.1	4.6	Lateritic Clay	
	443.6	25.6	30.2	Compacted sandstone	
	6273.0	53.1	83.3	Compacted sandstone	
14	2125.8	30.1	113.9	Sandstone/aquifer layer	AH
	5409.3			Sandstone	
	230.3	2.6	2.6	Top soil	
	710.7	1.4	4.0	Lateritic Clay	
	5876.9	19.0	23.0	Compacted sandstone	
15	1875.9	62.5	85.5	Sandstone/aquifer layer	HK
	18483.2			Sandstone	
	1024.0	0.4	0.4	Top soil	
	54.2	2.3	2.7	Lateritic Clay	
	1008.9	20.0	22.7	Compacted sandstone	
16	435.6	10.3	33.0	Sandstone/aquifer layer	A
	51.0			Sandstone	
	311.8	0.4	0.4	Top soil	
	969.8	4.4	4.8	Lateritic Clay	
	3004.0	2.0	6.8	Sandstone/aquifer layer	
	20616.0	3.9	10.7	Compacted Sandstone	
	10000.0			Compacted Sandston	

VES No.	Resistivity (Ω m)	Thickness (m)	Depth (m)	Lithology	Curve Type
17	228.9	6.3	6.3	Top soil	KH
	1218.7	6.9	13.2	Lateritic Clay	
	48.5	23.3	36.5	Sandstone/aquifer layer	
	2264.3			Compacted sandstone	
18	335.5	0.4	0.4	Top soil	AH
	1582.4	10.0	10.4	Lateritic Clay	
	5352.4	12.9	23.3	Compacted sandstone	
	6907.7	84.6	107.9	Sandstone/aquifer layer	
	5327.9			Sandstone	
19	226.0	0.4	0.4	Top soil	KH
	5609.7	1.9	2.2	Lateritic Clay	
	749.1	18.6	20.8	Sandstone/aquifer layer	
	5135.1	21.7	42.5	Compacted Sandstone	
	51103.2			Compacted sandstone	
20	298.2	0.4	0.4	Top soil	KH
	3527.4	2.7	3.2	Lateritic Clay	
	1145.5	2.9	6.1	Compacted sandstone	
	629.9	78.6	84.7	Sandstone/aquifer layer	
	1451.9	59.9	144.6	Compacted Sandstone	
	2742.3			Compacted Sandstone	
21	332.2	0.5	0.5	Top soil	KH
	528.4	7.0	7.0	Lateritic Clay	
	3837.5	10.2	17.1	Compacted sandstone	
	319.7	58.1	75.3	Sandstone/aquifer layer	
	1482.0			Sandstone	
22	132.7	0.8	0.8	Top soil	A
	301.1	4.2	5.0	Lateritic Clay	
	537.4	33.2	38.3	Sandstone/aquifer layer	
	30887.7	32.7	71.0	Compacted Sandstone	
	12307.5			Compacted Sandstone	
23	378.9	5.5	5.5	Top soil	KH
	1489.6	6.9	12.5	Lateritic Clay	
	31.8	20.6	33.1	Sandy clay	
	107.1	24.9	58.0	Sandstone/aquifer layer	
	663.3			Sandstone/shale	
24	302.8	1.2	1.2	Top soil	HA
	15.8	39.0	40.1	Lateritic Clay	
	79.3	17.0	57.2	Sandy clay	
	136.4	22.4	79.6	Sandstone/aquifer layer	
	399.1			Sandstone	
25	238.0	0.5	0.5	Top soil	KH
	1041.3	1.4	1.9	Lateritic Clay	
	11.0	16.4	18.2	Sandy clay	
	231.0	25.7	44.0	Sandstone/aquifer layer	
	918.7			Sandstone	
26	348.9	0.6	0.6	Top soil	KH
	799.8	3.9	4.5	Lateritic Clay	
	19.6	58.6	63.1	Sandy clay	
	24.0			Sandstone/aquifer layer	
27	346.7	1.7	1.7	Top soil	HK
	7.7	3.8	5.4	Lateritic Clay	
	67.2	11.3	16.8	Sandy clay	
	7.7	34.1	50.8	Claye sand/aquifer layer	
	64.2			Sandstone	

VES No.	Resistivity (Ω m)	Thickness (m)	Depth (m)	Lithology	Curve Type
28	381.8	5.5	5.5	Top soil	KH
	1592.6	6.7	12.2	Lateritic Clay	
	32.8	25.6	37.8	Sandy clay	
	235.5	27.7	65.5	Sandstone/aquifer layer	
	235.5			Sandstone	
29	318.7	3.7	3.7	Top soil	HA
	12.0	36.5	40.2	Lateritic Clay	
	29.9	21.0	61.2	Sandy clay	
	45.9	18.0	79.2	Sandstone/aquifer layer	
	265.5			Sandstone	
30	380.2	0.5	0.5	Top soil	KH
	1320.6	7.6	8.1	Lateritic Clay	
	8625.9	23.1	31.2	Compacted sandstone	
	1392.1	66.6	97.8	Sandstone/aquifer layer	
	2583.9			Compacted Sandstone	
31	262.8	1.8	1.8	Top soil	HA
	106.6	30.6	32.3	Lateritic Clay	
	802.6	19.0	51.3	Compacted sandstone	
	404.9	7.1	58.4	Sandstone/aquifer layer	
	3966.8			Compacted Sandstone	
32	387.0	0.7	0.7	Top soil	KH
	499.8	7.3	8.0	Lateritic Clay	
	14.4	44.5	52.5	Sandy clay	
	45.8	22.6	75.1	Clayey Sand/aquifer layer	
	270.7			Sandstone	
33	163.8	0.7	0.7	Top soil	KH
	318.3	1.3	20	Lateritic Clay	
	9.5	29.1	31.1	Clayey sand	
	20.5	45.8	76.9	Sandy clay/aquifer layer	
	27.6			Sandstone	
34	325.2	0.8	0.8	Top soil	HA
	2012.9	5.3	6.1	Lateritic Clay	
	2376.2	16.7	22.8	Compacted sandstone	
	56241.5	100.0	122.8	Compacted sandstone	
	7001.6	18.2	141.0	Sandstone/aquifer layer	
	15065.4			Compacted Sandstone	
35	212.2	2.4	2.4	Top soil	K
	2312.6	4.8	7.2	Lateritic Clay	
	4154.5	31.3	38.4	Compacted sandstone	
	553.5			Sandstone/aquifer layer	
36	345.0	2.9	2.9	Top soil	HA
	55.8	2.3	5.2	Lateritic Clay	
	28.7	8.2	13.3	Sandy clay	
	2.7	18.9	32.3	Clay	
	276.9			Sandstone/aquifer layer	
37	262.0	1.0	1.0	Top soil	KH
	4249.1	4.6	5.6	Lateritic Clay	
	1139.6	36.2	41.8	Sandstone/aquifer layer	
	1969.8	18.0	59.7	Compacted Sandstone	
	2885.0			Compacted sandstone	
38	204.8	0.4	0.4	Top soil	KH
	1748.9	2.6	3.0	Lateritic Clay	
	290.7	12.2	15.2	Sandstone	
	28805.4	85.8	101.1	Compacted sandstone	
	6823.5	27.8	128.7	Sandstone/aquifer layer	
	19801.3			Compacted Sandstone	

VES No.	Resistivity (Ω m)	Thickness (m)	Depth (m)	Lithology	Curve Type
39	402.9	1.4	1.4	Top soil	K
	2001.7	12.6	14.0	Lateritic Clay	
	21702.2	36.4	50.4	Compacted sandstone	
	8415.0	27.2	77.6	Sandstone/aquifer layer	
	5036.9			Sandstone	
40	374.9	1.1	1.1	Top soil	KH
	1284.5	5.7	6.7	Lateritic Clay	
	3740.8	19.5	26.2	Compacted sandstone	
	964.3	30.4	56.6	Sandstone/aquifer layer	
	1770.3	18.1	74.8	Compacted Sandstone	
	16098.1			Compacted Sandstone	

The major curve types are AK (VES 1), K (VES 2, 11, 35, and 39), HA (VES 3, 8, 24, 29, 31, 34, and 36), KH (VES 4, 5, 6, 9, 10, 12, 13, 17, 19, 20, 21, 23, 25, 26, 28, 30, 32, 33, 37, 38, and 40), A (VES 7, 16, and 22), AH (VES 14 and 18) and HK (VES 15 and 27).

The aquifer resistivity values range from 19.6 Ω m to 8986.9 Ω m with an average value of 1769.66 Ω m (Table 2). There is variation of resistivity value due to the difference lithology that characterized the area. Aquifer thickness values range from 2 to 84.6 m, with an average of 29.52 m (Table 2). Each type of rock has a different aquifer resistivity and thickness value, as shown in Table 1. Obasi et al. (2021, 2022) stated that, areas that are underlain by shales and poorly consolidated sandstones, their resistivity values are much lower than their older and highly consolidated counterparts. Also, low resistivity values in sandstones are often a function of porosity, clay type and content, temperature, salinity, dissolved heavy metal content and to a large extent the degree

of saturation (Ebong et al., 2014; Obrike et al., 2022). Therefore, the aquifer resistivity and thickness were used to classified the groundwater potential of the area. The classes are low, moderate and good groundwater potential with majority of the VES points within the moderate and good groundwater potential. Figure 4 is the aquifer resistivity map which showed that the majority of the area underlain by the Mamu formation in the southern part and part of the Ajali formation in the northwestern part of the study area is characterized by low resistivity value. This low resistivity value in the Mamu formation is as a result of clayey sand material while that of the Ajali formation may represent the unconsolidated sandstone with high porosity. Aquifer thickness map (Figure 5) indicated high value at the extreme of the eastern part and northwestern part of the study area which correlate mostly with areas underlain by the low resistivity value.

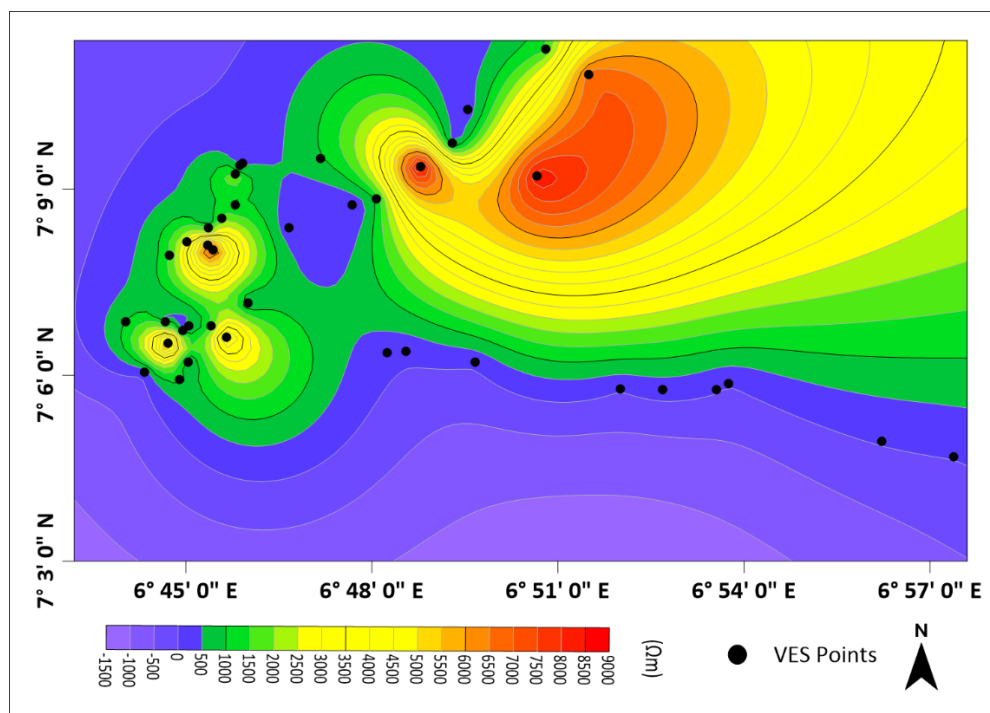


Figure 4: Aquifer Resistivity Map

The value of depth to groundwater varies from 6.8 m to 144.6 m with a mean value of 66.86 m indicating shallow aquifer depth for developing hand dug wells and deeper aquifer depth

for developing a motorized borehole (Table 2). Most of the deeper aquifer are found in an area underlain by the Ajali Sandstone in the research region (Figure 6).

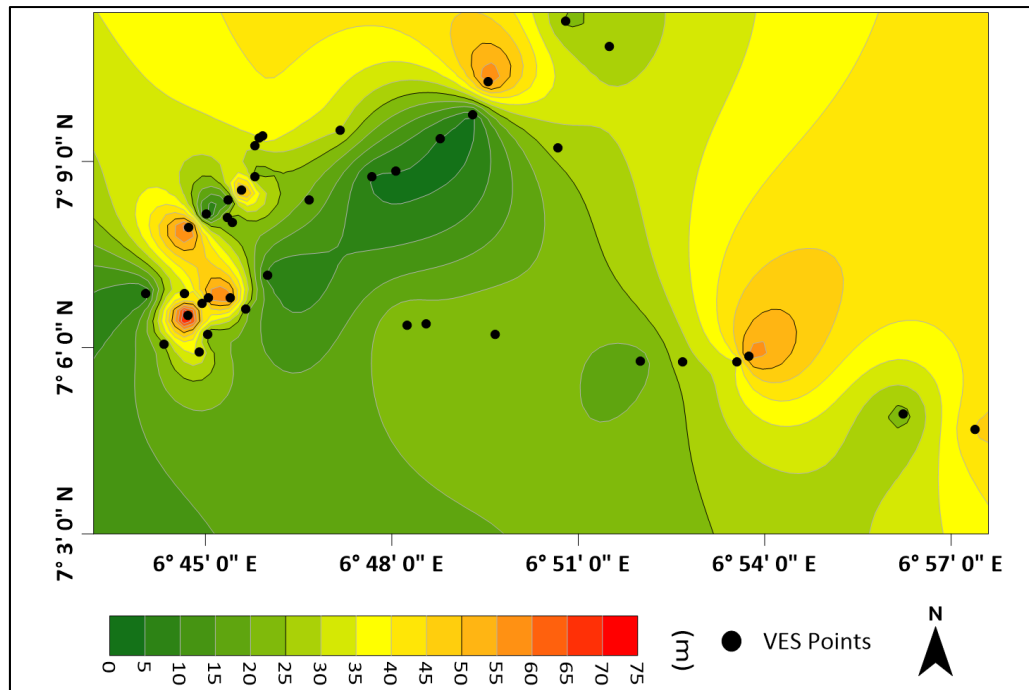


Figure 5: Aquifer Thickness Map

Table 2: Calculated Aquifer Properties from the Geoelectric Data

VES No.	Resistivity (Ωm)	Thickness (m)	Depth (m)	Lc (Siemens)	TR (Ωm^2)	K (m/day)	T (m^2/day)
Minimum	19.6	2	6.8	0.000523	435.2	0.079249	0.372468
Maximum	8986.9	84.6	144.6	2.989796	584391.4	24.07586	1410.846
Average	1769.66	29.52	66.85	0.245477	52860.83	3.619182	122.5311

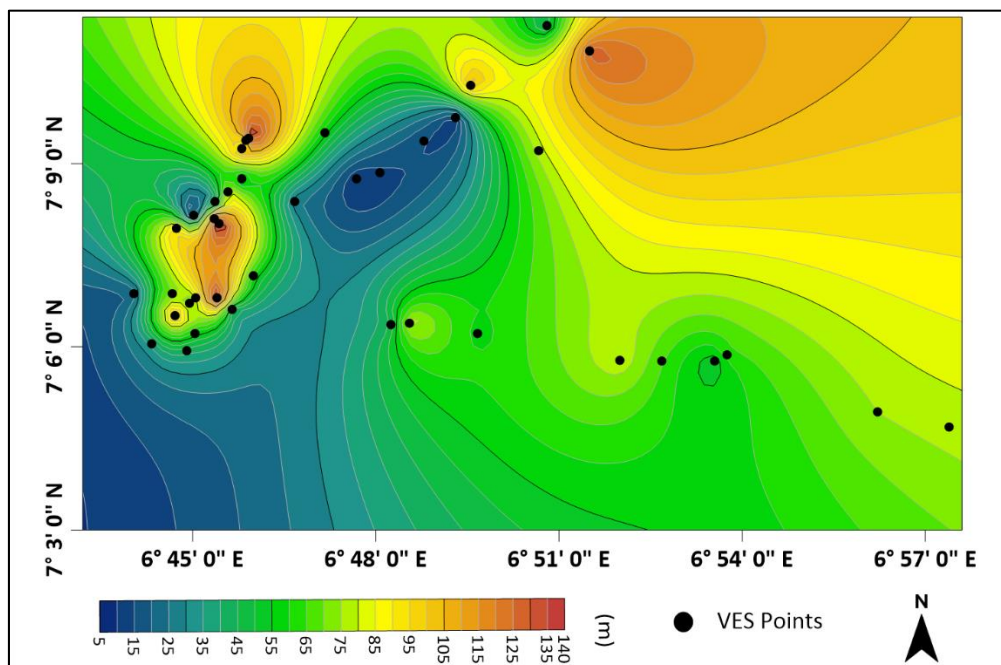


Figure 6: Aquifer Depth Map

Longitudinal conductance (Lc) has an average value of 0.2455 siemens with a range of 0.0052 to 2.9898 siemens (Table 2). The longitudinal conductance showed that the research region has low to high longitudinal conductance (poor to good protective capacity) using the classification scheme given in Table 3. This implies that regions with poor longitudinal conductance have a limited ability to protect, and

it also suggests that the local aquifer is vulnerable to contamination (Obasi *et al.*, 2022; Kizito *et al.*, 2023a; Hudu *et al.*, 2024). The longitudinal conductance map (Figure 7) showed a kind of diagonal increase from the southeast to the northwest within the study area which also indicated the area underlain by loose sandstone and clay has having high value.

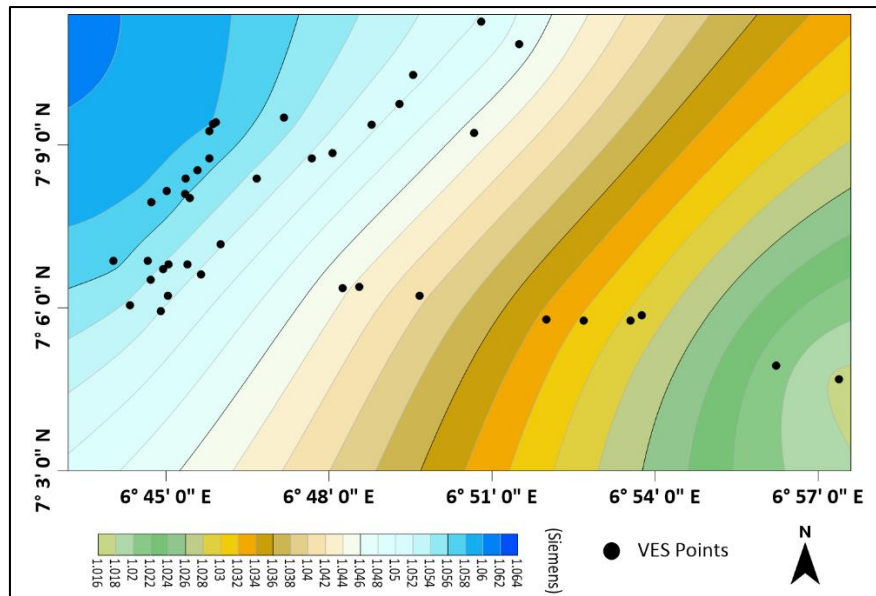


Figure 7: Longitudinal Conductance Map

The value of transverse unit resistance (T_r) ranges from 435.2 Ωm^2 to 584391.4 Ωm^2 with an average value of 52860.83 Ωm^2 (Table 2). Transverse resistance is a vital parameter that quantifies the opposition groundwater faces when flowing perpendicular to the hydraulic gradient through an aquifer (Akidi et al., 2024) and it is synonymous to aquifer yield

(Simon et al., 2022; Hudu et al., 2024). The transverse resistance map (Figure 8) showed low value at southern and few part of the northwestern region of the study area which correlate with what was revealed by the resistivity map of the study area.

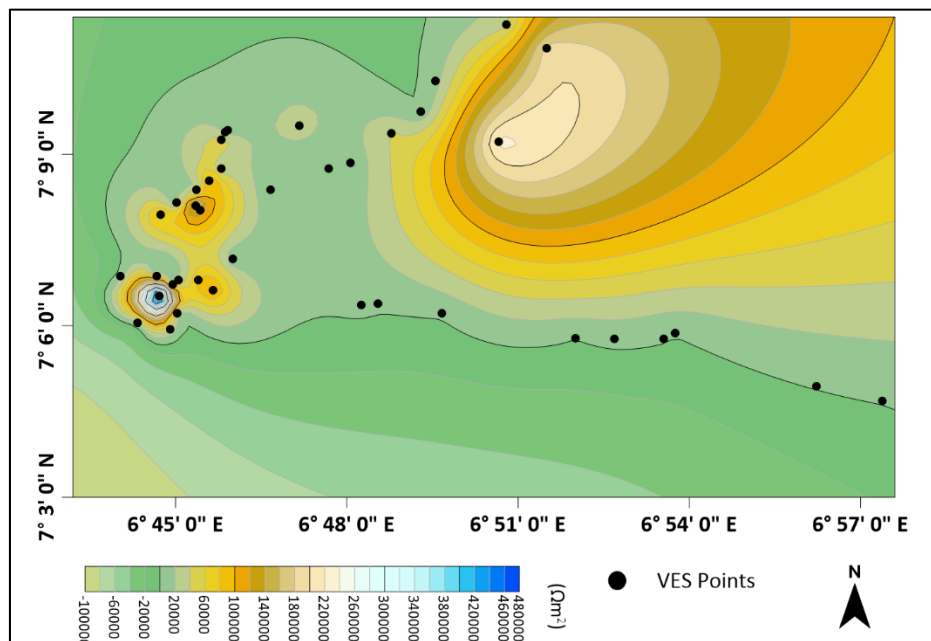


Figure 8: Transverse Resistance Map

Hydraulic conductivity (K) has value that ranges from 0.0793 m/day to 24.0759 m/day and mean value of 3.6192 m/day (Table 2). While the value of transmissivity (T) ranges from 0.3725 m^2/day to 1410.846 m^2/day with an average value of 122.5311 m^2/day (Table 2). Elevated hydraulic conductivity and transmissivity values signify a well-connected aquifer, enhanced permeability, and facilitated groundwater movement, ultimately leading to higher water yields. In contrast, poorly connected aquifer materials hinder groundwater flow, resulting in diminished yields (Opara et al., 2020). Based on the Krasny (1993) classification of

transmissivity (Table 4) indicated that study area has very low to very high groundwater classification with majority area having moderate to very high classes. The transmissivity map (Figure 9) showed that the extreme end of the eastern region of the study area is characterized by high to very high transmissivity value while the remaining area is dominated by low to moderate transmissivity value. This indicated that the extreme end of the eastern region has high permeability as compared to other areas and this is also seen in the hydraulic conductivity map (Figure 10).

Table 3: Aquifer Protective Capacity Ranges (Henriet, 1976; Oladapo *et al.*, 2004)

Longitudinal Conductance (mhom)	Protective Capacity Classification
>10	Excellent
5 - 10	Very good
0.7 - 4.9	Good
0.2 - 0.69	Moderate
0.1 - 0.19	weak
<0.1	poor

Table 4: Aquifer Transmissivity Classification (Krasny, 1993)

Transmissivity (m ² /day)	Classification	Groundwater Supply Potential
>1000	Very High	Great Regional Supply
100 - 1000	High	Lesser Regional Supply
10.0 - 100	Intermediate	Great Local Supply
1.0 - 10.0	Low	Smaller Local Supply
0.1 - 1.0	Very Low	Limited Local Supply
<0.1	Impermeable	Difficult Water Supply

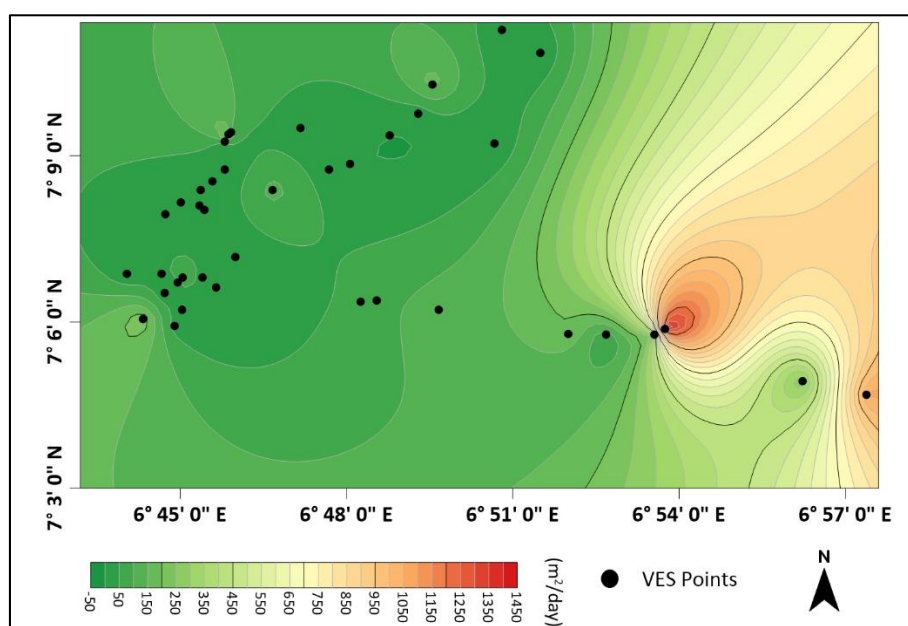


Figure 9: Transmissivity Map

CONCLUSION

The aquifer potential and protective capacity of Idah and its surroundings were assessed using data from Vertical Electrical Sounding (VES) and Dar-Zarrouk parameters, with the goal of informing sustainable water resources management practices. The geoelectric layer as revealed by VES graphs, showed four (4) to six (6) subsurface lithology with varying resistivity and thickness value. The layer includes the top soil, lateritic clay, compacted sandstone, Sandstone/clay/clayey sand, Aquiferous sandstone/sandy clay and highly compacted sandstone/shale as the case may be. The major curve types are AK, K, HA, KH, A, AH, and HK. The interpreted aquifer resistivity, showed that the southern and northwestern region is characterized by low value as a result of clayey and unconsolidated sandstone. This area with low aquifer resistivity also revealed high aquifer protective capacity and as such, the aquifers within this region has less groundwater contamination. Hydraulic conductivity and Transmissivity value indicated that the research region has groundwater potential class ranges from low to very high with the extreme eastern region having high to very high groundwater potential.

REFERENCES

- Adagunodo, T.A., Adeniji, A. A., Erinle, A., Akinwumi, S.A., Adewoyin, O.O., Joel, E.S., Kayode, O.T. (2017a). Geophysical Investigation into the integrity of a reclaimed open dumpsite for civil engineering purposes. *Interciencia Journal*, 42 (11), 324–339. <https://api.semanticscholar.org/CorpusID:59334808>
- Akiang, F. B., Amah, E. T., George, A. M., Okoli, E. A., Agbasi, O. E., Iwuoha, P. O. (2024). Hydrogeological Assessment and Groundwater Potential Study in Calabar South Local Government Area: A Vertical Electrical Sounding (VES) Approach. *International Journal of Energy and Water Resources*. <https://doi.org/10.1007/s42108-024-00279-y>
- Akidi, S. O., Ubechu, B. O., Obioha, Y. E., Ikechukwu, C. C. and Amadi, C. C. (2024). Geoelectrical Resistivity Mapping for Sustainable Groundwater Management in Umuahia South: Insights from vertical electrical sounding. *International Journal of Science and Research Archive*, 13 (01), 2296–2319. <https://doi.org/10.30574/ijrsra.2024.13.1.1922>

- Akpan, A. E., Ebong, D. E., Emeka, C. N. (2015). Exploratory Assessment of Groundwater Vulnerability to Pollution in Abi, southeastern Nigeria, using Geophysical and Geological Techniques. *Environ Monit Assess*, 187, 156. <https://doi.org/10.1007/s10661-015-4380-2>.
- Anandhi A., Kannan N. (2018). Vulnerability Assessment of Water Resources - Translating a Theoretical Concept to an Operational Framework using Systems Thinking Approach in a Changing Climate: Case Study in Ogallala Aquifer. *Journal of Hydrology*, 557, 460-474. <https://doi.org/10.1016/j.jhydrol.2017.11.032>
- Anudu, G. K., Essien, B. I. and Obrike, S. E. (2014). Hydrogeophysical Investigation and Estimation of Groundwater Potentials of the Lower Palaeozoic to Precambrian Crystalline Basement Rocks in Keffi area, North-Central Nigeria, using Resistivity Methods. *Arabian Journal of Geoscience* 7: 311–322. <https://doi.org/10.1007/s12517-012-0789-x>
- Bernard, J. (2003). Short Note on Depth of Investigation of Electrical Methods. Accessed 27 July 2016. www.iris-instruments.com
- Bolade, A. O., Bashir, A. O, Ojotejuto, F. U. and Moses, O. (2021). Assessment of the Water Quality of Hand Dug Wells in Idah, Kogi State, Nigeria. *FSD KSU journal*, 1 (1), 23-34. <https://www.researchgate.net/publication/355927133>
- Ebong, D. E., Akpan, A. E. and Onwuegbuche, A. A. (2014). Estimation of Geohydraulic Parameters from Fractured Shales and Sandstone Aquifers of Abi (Nigeria) using Electrical Resistivity and Hydrogeologic Measurements. *Journal of African Earth Sciences*. 96, 99–109. <https://doi.org/10.1016/j.jafrearsci.2014.03.026>
- Elbarbary, S., Araffa, S. A. S., El-Shaha, t A., Abdel Zaher, M., Khedher, K. M. (2021). Delineation of Water Potentiality Areas at Wadi El-Arish, Sinai, Egypt, using Hydrological and Geophysical Techniques. *Journal of African Earth Sciences*, 174, 6. <https://doi.org/10.1016/j.jafrearsci.2020.104056>
- Emenike, P. C., Nnaji, C. C., Tenebe, I. T. (2018). Assessment of geospatial and Hydrochemical Interactions of Groundwater Quality, Southwestern Nigeria. *Environmental Monitoring and Assessment*, 190(7). <https://doi.org/10.1007/s10661-018-6799-8>
- Eyankware, M. O., Okeke, G. C. (2018). Delineation of fracture in Ohofia Agba and it's Environs Ebonyi State, Southeastern Nigeria using Geographic Information System (GIS). *Discovery*, 54 (265), 1-12. www.discoveryjournal.com
- Henriet, J. (1976). Direct Applications of the Dar Zarrouk Parameters in Groundwater Surveys. *Geo. Pros.*, 24 (2), 344-53. <http://dx.doi.org/10.1111/j.1365-2478.1976.tb00931.x>
- Hudu, A. S., Fabian, A. A., Kizito, O. M. and Jacob, B. J. (2024). Application of Primary and Secondary Resistivity Parameters in Evaluating Aquifer Potential and Vulnerability Within Kabba, North Central Nigeria. *FUDMA Journal of Sciences (FJS)*, 8 (4), 221 – 234. <https://doi.org/10.33003/fjs-2024-0804-2581>
- Ileoje, A.J. (2001). "Climate of Nigeria's" CSS Bookshops Limtd, Lagos, P. 277 – 346.
- Kalaivanan, K., Gurugnanam, B., Suresh, M., Kom, K.P., Kumaravel, S. (2019). Geoelectrical Resistivity Investigation for Hydrogeology Conditions and Groundwater Potential Zone Mapping of Kodavanan Sub-basin, southern India. *Sustainable Water Resources Management*, 5, 1281–1301. <https://doi.org/10.1007/s40899-019-00305-6>
- Kizito, M. O., Obasi, I. A., Auduson, A. E., Jatto, S. S., Akudo, E. O., Akpah, F. and Jimoh, J. B. (2023b). Integrating Geoelectrical and Borehole Data in the Characterization of Basement-Rock Aquifers in the Lokoja area, Northcentral Nigeria. *Geosystems and Geoenvironment*, 2, 1-10. <https://doi.org/10.1016/j.geogeo.2023.100217>
- Kizito, O. Musa, Jamilu, B. Ahmed, Fabian, A. Akpah, Ernest, O. Akudo, Ikenna, A. Obasi, Solomon, S. Jatto, Andrew, C. Nanfa, Jacob, B. Jimoh (2023a). Assessment of groundwater potential and aquifer characteristics using inverted resistivity and pumping test data within Lokoja area, north-central Nigeria. *Communication in physical sciences*, 9 (3), 336 – 349. <https://journalcps.com/index.php/volumes/article/view/381>
- Krasny, J. (1993). Classification of Transmissivity Magnitude and Variation. Groundwater. *J. Assoc. Groundwater Scientists Eng.*, 31: 230-236. <https://doi.org/10.1111/j.1745-6584.1993.tb01815.x>
- Ladipo, K. O. (1986). Tidal Shelf Depositional Model for the Ajali Sandstone, Anambra Basin, Southern Nigeria. *Journal of African Earth Sciences*, 5(2), 177-185. <https://api.semanticscholar.org/CorpusID:129315912>
- Lukman, A. M., Ayuba, R. and Alege, Tope S. (2018). Sedimentology and Depositional Environments of the Maastrichtian Mamu Formation, Northern Anambra Basin, Nigeria. *Advances in Applied Science Research*, 9(2), 53-68. www.pelagiaresearchlibrary.com
- Nigm, A. A., Elterb R. A., Nasr, F. E., Thobaity, H. M. (2008). Contribution of Ground Magnetic and Resistivity Methods in Groundwater Assessment in Wadi Bany Omair, Holy Makkah Area, Saudi Arabia. *Egyptian Geophysical Society Journal*, 6, 67–79. <https://doi.org/10.21608/jegs.2008.380854>
- Nwajide, C. S. (2005). Anambra Basin of Nigeria: Synoptic Basin Analysis as a Basis for Evaluating its Hydrocarbon Prospectivity. Hydrocarbon Potentials of the Anambra Basin, PTDF Chair, 2-46. <https://www.scirp.org/reference/referencespapers?referenceid=2537995>
- Nwajide, C. S. (2013). Geology of Nigeria's Sedimentary Basins, CSS Bookshops Ltd, Lagos Nigeria. 451p. <https://www.scirp.org/reference/ReferencesPapers?ReferenceID=1551678>
- Obasi, A. I., Aigbadon, G. O., Chinyem, F. I., Chukwu, C. N., Ahmed, II J. B., Abubakar, S. O., Attah, F. D., Akudo, E. O. (2023). Estimation of Aquifer Parameters from Electrical Resistivity Data and Lithologs in Idah Area, Northern Anambra Basin, Nigeria. *Ife Journal of Science*, 25 (3), 457-469. <https://doi.org/10.4314/ijfs.v25i3.10>
- Obasi, I. A., Ahmed, II J. B., Aigbadon, G. O., Anakwuba, E. K., Akudo, E. O., & Onwa, N. M. (2022). Assessment of

Aquifer Vulnerability in the Tectonically Deformed Sedimentary Rocks in Abakaliki Area, Southeastern Nigeria, using Geophysical and Geological Data. *Environmental Earth Sciences*, 82. <https://doi.org/10.1007/s12665-023-10851-0>

Obasi, I.A., Nneka, M.O., Ezekiel, O.I. (2021). Application of the resistivity method in characterizing fractured aquifer in sedimentary rocks in Abakaliki area, southern Benue Trough, Nigeria. *Environmental Earth Science*, 80, 24. <https://doi.org/10.1007/s12665-020-09303-w>

Obrike, S. E., Oleka, A. B., Ojuola, B. S., Anudu, G. K., Kana, M. A. and Iliya, M. M. (2022). Hydro-Geophysical Assessment of Groundwater Potential and Aquifer Vulnerability of the Turonian Makurdi Formation in North Bank Area, Makurdi, Middle Benue Trough, Nigeria. *Journal of Mining and Geology*, 58 (1), 189-202. <https://www.researchgate.net/publication/36044847>

Okoli, E., Akaolisa, C. C. Z., Ubechu, B. O., Agbasi, O. E., Szafarczyk, A. (2024). Using VES and GIS-Based DRASTIC Analysis to Evaluate Groundwater Aquifer Contamination Vulnerability in Owerri, Southeastern Nigeria. *Ecological Questions*, 35(3), 1–27. <https://doi.org/10.12775/EQ.2024.031>

Oladapo, M. I., Mohammed, M. Z., Adeoye, O. O., & Adetola, B. A. (2004). Geoelectrical Investigation of the Ondo State Housing Corporation Estate, Ijapo Akure, Southwestern Nigeria. *J. of Min. and Geol.*, 40 (1), 41–48. <http://dx.doi.org/10.4314/jmg.v40i1.18807>

Olubayo, A. A. (2010). Hydrogeology of the Abeokuta Area, Southwestern Nigeria. *Journal of African Earth Sciences*, 56(2), 147-157.

Onyekuru, S. O., Achukwu-Ononye, O. U., Ukpong, A. J., Ofoh, I. J., Ibeneme, S. I., Ibe, K. K., Anyanwu, T. C. (2023). Stratigraphy and Paleoenvironment (s) of the Late Cretaceous Deposits in Ohafia Area, Afikpo Basin, Southeastern Nigeria. *Journal of African Earth Sciences*, 197, 104713. <https://doi.org/10.9790/1813-0602021930>

Opara, A. I., Eke, D. R., Onu, N. N., Ekwe, A. C., Akaolisa, C. Z., Okoli A. E., & Inyang, G. E. (2020). Geo-hydraulic Evaluation of Aquifers of the Upper Imo River Basin, Southeastern Nigeria using Dar-Zarrouk parameters. *International Journal of Energy and Water Resources*, 5(3), 259–275. <https://doi.org/10.1007/s42108-020-00099-w>

Orellana, E. and Mooney, H. (1966). Master Tables and Curves for VES over Layered Structures. Interciencia, Madrid, Spain. <https://www.scirp.org/reference/referencespapers?referenceid=2602987>

Preeja, K. R., Sabu, J., Jobin, T., Vijith, H. (2011). Identification of Groundwater Potential Zones of a Tropical River Basin (Kerala, India) Using Remote Sensing and GIS Techniques. *Journal of the Indian Society of Remote Sensing*, 39(1), 83-94. <https://doi.org/10.1007/s12524-011-0075-5>

Simon, S. S., Ishaku, J. M., Seli, A. B., Boniface, F. (2022). Evaluation of Groundwater Potentials Using Dar Zarrouk Parameters in Mapeo and Environs, North-Eastern Nigeria. *Dutse Journal of Pure and Applied Sciences (DUJOPAS)*, 8 (3b), 124-135. <https://doi.org/10.4314/dujopas.v8i3b.13>

Singh, L. K., Jha, M. K., Chowdary, V. M. (2018). Assessing the Accuracy of GIS-based Multi-Criteria Decision Analysis Approaches for Mapping Groundwater Potential. *Ecological Indicators*, 91, 24-37. <https://doi.org/10.1016/j.ecolind.2018.03.059>

Thabit J. M., Al-hameedawie M. M. (2014). Delineation of Groundwater Aquifers using VES and 2D Imaging Techniques in north Badra Area, Eastern Iraq. *Iraqi Journal of Science*, 55, 174–183. <https://www.researchgate.net/publication/267249337>

Whiteman, A. J. (1982). Nigeria; its Petroleum Geology, Resources and Potentials. Graham and Trotman, London, 394p. <http://dx.doi.org/10.1007/978-94-009-7361-9>

Yusuf, I., Obaje, N. G., Adedosu, T. A., Adeoye, J. A., Adamu, L. M., Tsado, F. and Gana, E. Y. (2023). Geology, Sedimentological and Hydraulic Conductivity of Ajali Potential Reservoir Sandstone Exposed Around Gra in Idah, Northern Anambra Basin. *FUDMA Journal of Sciences (FJS)*, 7 (6), 290 – 297. <https://doi.org/10.33003/fjs-2023-0706-2129>

Zohdy, A. A. R., Eaton, G. P., Mabey, D. R. (1974). Application of Surface Geophysics to Ground-water Investigations. *Techniques of Water-Resources Investigations of the United States Geological Survey* 2, 123. <https://www.scirp.org/reference/referencespapers?referenceid=2157743>



©2024 This is an Open Access article distributed under the terms of the Creative Commons Attribution 4.0 International license viewed via <https://creativecommons.org/licenses/by/4.0/>, which permits unrestricted use, distribution, and reproduction in any medium, provided the original work is cited appropriately.